Promising Cytotoxic butenolides from the Soybean endophytic fungus *Aspergillus terreus:* A combined molecular docking and In-vitro studies

Seham S. El-Hawary[1], Abeer S. Moawad[2], Hebatallah S. Bahr[3], Eman Z. Attia[4], Mo`men H. El-Katatny[5], Muhamad Mustafa[6,7], Ahmed A. Al-karmalawy[8], Mostafa E. Rateb[9], Jian-ye Zhang[10], Usama Ramadan Abdelmohsen[11*] and Rabab Mohammed[2*]

[1] Department of Pharmacognosy, Faculty of Pharmacy, Cairo University, Cairo, Egypt

[2] Department of Pharmacognosy, Faculty of Pharmacy, Beni-Suef University, Beni-Suef, Egypt

[3] Department of Pharmacognosy, Faculty of Pharmacy, Nahda University, Beni-Suef, Egypt; Hebatallah.samir@nub.edu.eg

[4] Department of Pharmacognosy, Faculty of Pharmacy, Minia University, Minia, Egypt

[5] Department of Botany and Microbiology, Faculty of Science, Minia University, Minia, Egypt.

[6] Department of Medicinal Chemistry, Faculty of Pharmacy, Deraya University, 61111 New Minia, Egypt. muhamad_mustafa99@yahoo.com

[7] IBMM, Univ. Montpellier, CNRS, ENSCM, Montpellier, France.

[8] Pharmaceutical Chemistry Department, Faculty of Pharmacy, Ahram Canadian University, 6th of October City, Giza 12566, Egypt. akarmalawy@acu.edu.eg

[9] School of Computing, Engineering & Physical Sciences, University of the West of Scotland, Paisley PA1 2BE, UK; mostafa.rateb@uws.ac.uk

[10] Guangzhou Municipal and Guangdong Provincial Key Laboratory of Molecular Target & Clinical Pharmacology, the NMPA and State Key Laboratory of Respiratory Disease, School of Pharmaceutical Sciences and the Fifth Affiliated Hospital, Guangzhou Medical University, Guangzhou 511436, China; Jianyez2003@gmail.com

[11] Department of Pharmacognosy, Faculty of Pharmacy, Deraya University, 61111 New Minia City, Minia, Egypt; Usama.ramadan@mu.edu.eg

*__Corresponding authors:__ Rabab Mohammed (rmwork06@yahoo.com); Usama Ramadan Abdelmohsen (Usama.ramadan@mu.edu.eg).

Short running head: Cytotoxic butenolides from *A. terreus*.

Abstract

Aim: This study aimed to use one strain many compounds approach (OSMAC) to investigate the cytotoxic potential of *Aspergillus terreus* associated with soybean versus several cancer cell lines, by means of *in-silico* and *in vitro* approaches.

Methods and results: Fermentation of the isolated strain was done on five media. The derived extracts were investigated for their inhibitory activities against three human cancer cell lines; mammary gland breast cancer (MCF-7), colorectal adenocarcinoma (Caco-2) and hepatocellular carcinoma (HepG2) using MTT Assay. The fungal mycelia fermented in Modified Potato Dextrose Broth (MPDB) was the most cytotoxic extract against HepG2, MCF-7 and Caco-2 cell lines with IC_{50} 4.2 ±0.13, 5.9 ±0.013 and 7.3 ±0.004 µg.mL^{-1}, respectively. MPDB extract was scaled up resulting in the isolation of six metabolites; three fatty acids (**1, 2** and **4**), one sterol (**3**) and two butenolides (**5** and **6**) by column chromatography. The isolated compounds (**1-6**) were screened through a molecular docking approach for their binding aptitude to various active sites. butyrolactone-I **(5)** revealed a significant interaction within the CDK2 active site, while aspulvinone E **(6)** showed promising binding affinity to FLT3 and EGFR active sites that was confirmed by *in vitro* CDK2, FLT3 and EGFR inhibitory activity. Finally, the *in vitro* cytotoxic activities of butyrolactone-I (**5**) and aspulvinone E (**6**) revealed the antiproliferative activity of butyrolactone-I (**5**), against HepG2 cell line (IC_{50} = 17.85 ±0.32 µM).

Conclusion: Molecular docking analysis and *in vitro* assays suggested the CDK2/A2 inhibitory potential of butyrolactone-I (**5**) in addition to the promising interaction abilities of aspulvinone E (**6**) with EGFR and FLT3 active sites as a possible mechanism of their biological activities.

Significance and Impact of the Study: *Aspergillus terreus* extracts exhibited *in vitro* cytotoxic potential owed to their enrichment with biologically active metabolites. Hence, they are strongly recommended to be explored for possible anticancer compounds.

Keywords: Docking study; butyrolactone-I; aspulvinone E, Cdk2; FLT3; EGFR.

Abbreviations:

Cdk2: Cyclin-dependent kinases

FLT3: Fms-like Tyrosine Kinase 3

EGFR: Epidermal Growth Factor Receptor

Introduction

Cancer is a complex disease characterized by abnormal cellular growth (El-Hawary et al., 2021; Ahmed et al., 2021; Abdelaleem et al., 2022). Cancer cells showed uncontrolled replicative potential, high invasive ability and apoptotic resistance, making this disease the major cause of death worldwide (Uzma et al., 2018; Shady et al., 2021). On the other hand, patients treated from different types of cancer are suffering, because most of the available anticancer drugs display toxicity to proliferating normal cells, have severe side effects, and are less effective against several types of cancer (Youssif et al., 2020). In addition, certain types of cancer showed drug resistance (Kharwar et al., 2011). Therefore, the search for promising cytotoxic agents that improve the patient outcomes have always attracted the attention of researchers and scientists. Chemotherapies targeting the signaling pathways that control the tumor cell cycle and its microenvironment, inducing cell death, decreasing tumor cell proliferation or inhibiting tumor mass growth, have recently been investigated (Allam et al., 2020). Cyclin-dependent kinases (CDKs) and Receptor tyrosine kinases (RTKs) are among the well-studied molecular targets that regulate cell signaling pathways. CDKs are a family of serine/threonine protein kinases involved in numerous physiological processes that control the cell cycle (Abd El-Karim et al., 2019). Different CDKs (1-7) are only active when coupled to their regulator proteins, namely cyclins A-H (Lees, 1995). For cell division to be successful, CDK activity must be strictly regulated. Controlling CDK activity has been proven to be a promising treatment method for cancer pathophysiology since aberrant cell division is a hallmark of the disease. Cdk2/A2 complex, in particular, plays an important role in DNA replication, implying that Cdk2/A2 complex could be a plausible biological target for newly developing anticancer therapies (Lees, 1995; Abd El-Karim et al., 2019). On the other hand, RTKs (receptor tyrosine kinases), such as FLT3 and EGFR, are a family of

transmembrane proteins that play a role in signal transduction. They promote a wide range of cellular functions. Tumor cells frequently use these pathways to improve tumor growth and spread in malignancies. RTKs inhibitors are thus logical targets for the development of new anticancer drugs (Haluska and Adjei, 2001; Gary Gilliland and Griffin, 2002).

Natural products have a strong record of achievement in developing anticancer agents, which has led researchers and drug discovery programs to explore this rich source of molecular scaffolds (Elmaidomy et al., 2019; Owis et al., 2020; Sayed et al., 2020). Plant endophytes are one of the promising sources of anticancer natural products. Endophytes are fungi or bacteria that spend the whole or part of their life cycle colonizing inside the healthy tissues of the host plants without causing apparent symptoms of disease. The rich chemical diversity of endophytes natural products and their pronounced biological activities continue to thrill natural product chemists, ecologists and pharmacologists alike. Approximately 100 compounds with demonstrated anticancer activity have been isolated from endophytic fungi, including several compounds originally found in other higher plants (Kharwar et al., 2011). In addition, endophytes can be grown in large fermenters, producing unlimited supply of the desired metabolites which ensure their availability. *Aspergillus* is one of the most familiar filamentous fungi that belongs to Ascomycetes (Orfali et al., 2021). The endophytic *Aspergillus* species are renewable, inexhaustible sources of bioactive secondary metabolites, such as sterols, alkaloids, butenolides and cytochalasins, which are of great importance in pharmaceutical and commerical industries (Wang et al., 2018; El-hawary et al., 2020). *Aspergillus terreus* is a commonly isolated endophytic fungus, and is well-known for its unique metabolites as itaconic acid and the antihypercholesterolemic drug lovastatin, in addition to the antibiotics sulochrin and terrein (Elkhayat et al., 2015). Recently, *Aspergillus terreus* associated with the roots of soybean was reported for production of extracellular hydrolytic

enzymes such as carboxymethyl cellulose, xylanase, and amylase (Farouk et al., 2020). In our previous study, *Aspergillus terreus*, an endophyte hosted in soybean, was isolated, identified and cultivated in five media, including Potato Dextrose Broth (PDB), Modified Potato Dextrose Broth (MPDB), Sabouraud Broth (SAB), Malt Extract Broth (MEB), and Rice Extract Broth (REB), which were used for the fermentation of the isolated strain using one strain many compounds (OSMAC) approach to find the optimal media for fermentation and production of secondary metabolites. According to our earlier work, metabolomics and multivariate analysis revealed that Potato Dextrose Broth (PDB) and Modified Potato Dextrose Broth (MPDB) were the optimal media for fungal growth and metabolites production (El-Hawary et al., 2021). Hence, in continuance of our interest in such valuable strain, the present study describes the cytotoxic potential of different extracts derived from the OSMAC approach against human hepatoma (HepG2), human breast adenocarcinoma (MCF-7) and human colon adenocarcinoma (Caco-2) cell lines. In addition, isolation and structure elucidation of the major constituents afforded from the most cytotoxic active extract were achieved. Moreover, the isolated compounds (**1-6**) were screened and compared through a molecular docking approach for their binding aptitude to various active sites of cyclin-dependent kinases (CDKs) and receptor tyrosine kinases (RTKs), including PIM, EGFR, VEGFR, FLT3, Cdk2, Cdk9, FAK, P53 and tubulin as known validated targets for controlling cytotoxicity. Furthermore, *in vitro* enzymatic assays against Cdk2/A2, EGFR, and FLT3 as well as *in vitro* cytotoxic assays were performed on the compounds that showed strong binding affinities to specific active sites in order to confirm their enzyme inhibitory effects.

Materials and methods

General Experimental Procedures

The chemical solvents used in this study, such as *n*-hexane, dichloromethane, ethyl acetate and methanol, were obtained from Sigma-Aldrich (Saint Louis, Missouri, USA). Silica gel 60 (Fluka; 70–230 mesh, Sigma-Aldrich, Germany) and Sephadex LH-20 (0.25 mm; Sigma-Aldrich, Germany) were used for chromatographic isolation and purification. Thin-layer chromatography was performed using precoated silica gel 60 GF_{254} plates (E. Merck Darmstadt, Germany; 0.25 mm thick). Spraying reagent consisting of *p*-anisaldehyde-methanol-glacial acetic acid-sulfuric acid (0.5:85:10:5) was used as visualizing spray reagent for different spots accompanied by heating at 110°C. 1D and 2D-NMR experiments were recorded on a JEOL ECA-500 spectrometer (500 MHz for ^{1}H and 125 MHz for ^{13}C), and NMR Bruker Avance III spectrometer (400 MHZ for ^{1}H and 100 MHZ for ^{13}C). Each sample was dissolved in deuterated solvents, such as $CDCl_3$, DMSO-d_6 and CD_3OD (Sigma-Aldrich, Germany). All chemical shifts were recorded and expressed in δ ppm units related to the TMS signal as an internal standard and/or solvent residual proton signals, and coupling constants (*J*) were recorded in Hz.

Plant material

Plant materials were collected, identified and preserved as previously described by El-Hawary et al (El-Hawary et al., 2021).

Endophytic fungal Isolation

Our earlier study concerning the isolation of endophytic fungi from soybean included the isolation of the endophytic fungus *A. terreus* GMEF1 (Farouk et al., 2020).

Molecular Identification and phylogenetic analysis

Taxonomic identification of the isolated fungal strain recovered from the *Glycine max* L. root, was previously described by El-Hawary et al (El-Hawary et al., 2021).

Fungal Fermentation and Extract Preparation

By placing segments of fresh growing agar culture in 5 L Erlenmeyer flasks, the isolated sub-cultured *Aspergillus terreus* GMEF1 was fermented in 1.5 L different media, including PDB (Potato Dextrose Broth), MPDB (Modified Potato Dextrose Broth), Sabouraud Broth (SAB), Malt Extract Broth (MEB), and Rice Extract Broth (REB). The flasks were incubated at 20 °C under static circumstances for four weeks. To terminate the fermentation process, 300 mL of ethyl acetate was added to each flask at the end of fermentation. For PDB, MPDB, SAB, MEB, and REB, the fungal mycelia and culture broth were subjected to three ultrasound-assisted extractions with ethyl acetate (300 mL) to yield five culture broth ethyl acetate extracts (E1, E2, E4, E5, and E7) and five fungal mycelia methanolic extracts (J3, J4, J6, J7, and J9), respectively. After that, a rotary evaporator (Buchi Rotavapor R-300, Germany) was used to concentrate these extracts.

Isolation and Purification of Induced Metabolites

The extract of fungal mycelia derived from the fermentation of isolated strain on MPDB medium (J4) was scaled up (fermented in 5L broth) to afford 3 g dried extract. Such residue was dissolved in 10% MeOH and subjected to defatting by partitioning with *n*-hexane in a separating funnel. The *n*-hexane soluble fraction (1.8 g) was concentrated and subjected to further fractionation on silica gel (90 g) open column chromatography (2.5 cm × 75 cm); elution started with (*n*-hexane-DCM 90:10) followed by a gradient elution started with 100% DCM and increasing the polarity by 5% EtOAc till 100% EtOAc was reached, and washing was carried out by MeOH. A hundred mL fractions were collected to afford three main fractions (F1–F3). Fraction F1 (200 mg) was further fractionated on a silica gel column chromatography (15 g, 1.5 cm × 110 cm) using *n*-hexane-EtOAc gradient mixtures to finally provide compound **1** (20 mg). Fraction F2 (40 mg) was further fractionated on a silica gel column chromatography (5 g, 1×40 cm), using *n*-hexane-EtOAc gradient mixtures to yield compound **2** (10 mg). Fraction F3 (140 mg) was chromatographed on a

184 silica gel column chromatography with *n*-hexane-EtOAc gradient mixtures to provide two sub-
185 fractions (F3-I & F3-II). Pure needle crystals of compound **3** (8 mg) were precipitated from sub-
186 fraction F3-I (30 mg). F3-II (20 mg) was further chromatographed on silica gel using *n*-hexane-
187 EtOAc gradient mixtures as a mobile phase to afford pure compound **4** (7 mg). On the other hand,
188 the methanol soluble portion (1.2 g) was fractionated on open column chromatography using silica
189 gel (100 g, 2.5×75 cm) as stationary phase and eluted with *n*-hexane, DCM, EtOAc and MeOH as
190 mobile phase in gradient elution, started with 100% *n*-hexane, then 10% increment of DCM till
191 100% DCM, then 5% increment of EtOAc till 100% EtOAc reaching to 100% MeOH. Fifty mL
192 fractions were collected, and pooled in accordance to the TLC, using UV lamp and the spraying
193 reagent, *p*-anisaldehyde, followed by heating at 100ºC to finally provide 10 fractions (M1-M10).
194 Two fractions, M1 and M4, were found to be promising and are therefore subjected to further
195 chromatographic study. Fraction M1 (eluted with DCM: EtOAc 60%: 40%) was chromatographed
196 on a Sephadex LH-20 column (20 g, 1.5×110 cm) using DCM-MeOH (50:50) as mobile phase
197 yielding sub-fractions I and II. Sub-fraction II was further chromatographed on Sephadex LH-20
198 (5 g, 1x40 cm) using DCM-MeOH (50:50) to finally afford compound **5** (100 mg). Fraction M4
199 (eluted with 100% EtOAc) was chromatographed on a Sephadex LH-20 column (20 g,1.5×110
200 cm) using 100% MeOH as a mobile phase to give compound **6** (50 mg).

201 **Cytotoxic activity of the extracts**

202 MTT Assay was performed using different human cancer cell lines, including mammary gland
203 breast cancer (MCF-7), colorectal adenocarcinoma (Caco-2) and hepatocellular carcinoma (HepG-
204 2). The cell lines were purchased from the American Type Culture Collection (ATCC, Rockville,
205 MD, USA; HPACC, Salisbury, UK). Doxorubicin was used as a positive control. The cell lines
206 were used to detect the inhibitory effects of the extracts on cell growth. Cell viability was

determined via colorimetric assay (MTT), which is based on transforming the yellow tetrazolium bromide to purple formazan by mitochondrial succinate dehydrogenase. Cell lines were cultivated in rpmI-1640 medium supplemented with 10% fetal bovine serum, 100 units/mL penicillin, and 100 µg/mL streptomycin incubated at 37 ºC under 5% CO_2. The cell lines were plated in a 96 well microliter plate at a concentration of 1.0-10^4 cells/well and incubated at 37 ºC under 5% CO_2 for 2 days. Subsequently, the cells were mixed with different concentrations of the extracts and incubated for a further 24 h, and then treated with 20 mL of MTT solution at a concentration of 5 mg/mL and incubated for 4h. The purple formazan precipitates were dissolved in 100 mL of dimethyl sulfoxide (DMSO), and the optical density for each well was measured and recorded at an absorbance of 570 nm using a plate reader (EXL 800, Biotek®, Winooski, Vermont, USA). The relative cell viability as a percentage was calculated as A570 of treated samples/A570 of untreated sample x 100.

Docking analysis

The X-ray crystal protein structures were retrieved from the PDB using the Molecular Operating Environment software (MOE 2019.01, Chemical Computing Group, Montreal, QC, Canada) (Elmaaty et al., 2022). The QuickPrep module in the MOE software was employed to prepare all the protein structures utilized in this docking study (Elebeedy et al., 2021; Elebeedy et al., 2022). The chemical structures were drawn using the MOE build suite, and then energy was minimized using the MOE default forcefield as described earlier (Shoala et al., 2021; Mahmoud et al., 2022). The inessential ligands and water were cleared before docking. The native ligand in each co-crystal protein was taken as a center for the docking calculation grid. To validate the present study at the active sites, the co-crystallized ligands were re-docked into their active sites using the same set of parameters as described above (Mahmoud et al., 2021). The RMSD values of the best-docked pose

were less than 2 Å. The generated docking poses were classified according to their binding interactions and their binding free energy, and visualized with MOE software (Khattab and Al-Karmalawy, 2021).

In vitro Cdk2/ A2 enzyme assay

The Kinase-Glo® MAX Assay is a luminous kinase assay that detects the amount of ADP produced during a kinase process. ADP is transformed to ATP, which is then turned to light. The amount of ADP and the kinase activity are both positively correlated with the luminous signal. The assay was carried out according to the instructions included in the Cdk2/CyclinA2 Kinase Assay Kit, Promega Cat. #V6071, and included the following steps: 1st; the master mixture was prepared as follow: a) 6 µl 5x Kinase assay buffer 1. b) 1 µL of ATP solution (500 µM). c) 5 µl of Cdk substrate peptide 1. d) 13 µL distilled water, and then 25 µL of the master mixture was added to every well. 2nd; 5 µL of inhibitor solution was added to each well labeled as "Test Inhibitor", for the "Positive control" and "Blank", 5 µL of the same solution was added without inhibitor. 3rd; 3ml of 1x Kinase assay buffer was prepared by mixing 600 µL of 5x Kinase assay buffer 1 with 2400 µL water. Cdk2/Cyclin A2 enzyme was added on ice and diluted to ~5 ng/ µL with 1x Kinase assay buffer. The reaction was initiated by adding 20 µL of diluted Cdk2/Cyclin A2 enzyme to the wells designated as "Positive control" and "Test Inhibitor control" and then incubated at 30˚c for 45 min. plate was then incubated at room temperature for 15 minutes after adding 50 µL of Kinase-Glo® MAX reagent. Finally, for each concentration of the isolated compound (**5**) (0.01-10 $ng.mL^{-1}$), the luminescence was measured using the microplate reader. By comparing the percent inhibition of the samples to the log conc, the activity of the tested enzyme in the samples is determined. From dose-response curves, the concentration of the test drugs required to inhibit kinase activity by 50% was calculated and reported as their IC_{50}. [1]

***In vitro* EGFR kinase assay**

The assay was carried out according to the instructions included in the EGFR Kinase Assay Kit, Promega Cat. #40321 using Kinase-Glo® MAX (Promega #V6071) as a detection reagent and included the following steps, 1st: the master mixture (25 µL per well) was prepared by adding: a) 6 µL 5x Kinase assay buffer, b) 1 µL ATP (500 µM), c) 1 µL 50x PTK substrate, and d) 17 µL water, then 25 µL of the mixture was added to every well. 2nd: 5 µL of inhibitor solution added to each well labeled as "Test Inhibitor". For the "Positive Control" and "Blank", 5 µL of the same solution without inhibitor (Inhibitor buffer) was added. 3rd: 3 mL of 1x Kinase assay buffer was prepared by mixing 600 µL of 5x Kinase assay buffer with 2400 µL water. To the wells designated as "Blank", 20 µL of 1x Kinase assay buffer added. After that, EGFR enzyme was diluted to 1 $ng.mL^{-1}$ with 1x Kinase assay buffer. Reaction initiated by adding 20 µL of diluted EGFR enzyme to the wells designated "Positive Control" and "Test Inhibitor Control" and then incubated at 30°C for 40 minutes. After 40 minute reaction, 50 µL of Kinase-Glo Max reagent was added to each well. Plate covered with aluminum foil and incubated at room temperature for 15 minutes. Luminescence was measured for each concentration of the isolated compound (**6**) (0.01-10 $ng.mL^{-1}$) using the microplate reader.

***In vitro* FLT3 kinase assay**

FLT3 kinase inhibitory activity as measured by FLT3 kinase assay using ADP-Glo® Kinase Assay (Promega #V6930). The assay was carried out according to the FLT3 Kinase Assay Kit's instructions as follow: 1st: the master mixture was prepared by adding (3 µL 5x Kinase assay buffer + 0.5 µL ATP (500 µM) + 1 µL MBP (5 mg/ml) + 5.5 µL water). 10 µL of the mixture was added to every well. 2nd: 2.5 µL inhibitor solution was added to each well labeled as "Test Inhibitor". While, For the "Positive Control" and "Blank", 2.5 µL of the same solution was added without

inhibitor (Inhibitor buffer). 3rd: 3 mL of 1x Kinase assay buffer was prepared by mixing 600 µL of 5x Kinase assay buffer with 2400 µL water. To the wells designated as "Blank," add 12.5 µL of 1x Kinase assay buffer. 4th: the amount of FLT3 required for the assay was calculated and diluted to 1.5 ng/ µL with 1x Kinase assay buffer. The reaction was initiated by adding 12.5 µL of diluted FLT3 enzyme to the wells designated “Positive Control” and "Test Inhibitor Control", and incubated at 30°C for 45 minutes. After the 45 minutes reaction, 25 µL of ADP-Glo reagent added to each well. The plate was covered with aluminum foil and incubated at room temperature for 45 minutes. After 45 minutes incubation, 50 µL of Kinase Detection reagent was added to each well. The plate was covered with aluminum foil and incubated for another 45 minutes at room temperature. The sample was quantified immediately using a luminometer for each concentration of the isolated chemical (**6**) (0.01-10 ng.mL^{-1}). “Blank” value subtracted from all readings.

***In vitro* cytotoxicity of the active compounds.**

Experiments were carried out using MTT assay on the three human cancer cell lines, hepatocellular carcinoma (HepG-2), mammary gland breast cancer (MCF-7), and colorectal adenocarcinoma (Caco-2) as described by Allam *et al*., (Allam et al., 2020). The cell lines were purchased from the American type collection (ATCC, Rockville, MD, USA; HPACC, Salisbury, UK). Staurosporine was used as a positive control. After incubating the cancer cells with various concentration, doses in dimethyl sulfoxide (DMSO) ranging from (1, 10, 100, and 1000 g.mL^{-1}) for 48 hours, the vitality of the cancer cells was evaluated using 3-[4,5-methylthiazol-2-yl].2,5-Diphenyltetrazolium Bromide (MTT). Cells in the log phase of growth were used for the best outcomes, and each test included a blank that included entire media without cells. 10% of the culture medium volume worth of reconstituted MTT was added. Depending on the cell type and maximal cell density, cultures were placed back in the incubator for 2-4 hours. After the cultures had been incubated,

the incubator was shut off, and the formazan crystals that had formed were eliminated by adding MTT Solubilization Solution [M-8910] in a quantity equal to the volume of the original culture media and gently mixing. At a wavelength of 570 nm, absorbance was determined spectrophotometrically.

Statistical analysis

The data was displayed as mean and standard error of the mean. To analyze the data, Dunnett's test was used after one-way analysis of variance (ANOVA). GraphPad Prism 5 software was used to accomplish the statistical analysis (Version 5.01, San Diego, CA, USA). Results were considered as significant at $p < 0.05$.

Results

Cytotoxic activity

The cytotoxic activity of the ten fungal extracts of *A. terreus* against three-cancer cell lines (HepG2, MCF-7 and Caco-2) was evaluated **(Table 1)**, **(Fig.1)**. Results revealed that six extracts displayed cell growth inhibition against HepG2, MCF-7 and Caco-2. J4 and J3 extracts showed the highest cytotoxic activities against the tested cell lines, followed by E5 extract. Extract J4 displayed strong cytotoxicity against HepG2, MCF-7 and Caco-2 with IC_{50} 4.2 ±0.13, 5.9 ±0.013 and 7.3 ±0.004 $\mu g.mL^{-1}$, respectively. J3 displayed good cytotoxicity against HepG2, MCF-7 and Caco-2 with IC_{50} 5.6 ±0.15, 6.8 ±0.09 and 8.4 ±0.06 $\mu g.mL^{-1}$, respectively. Finally, E5 displayed good cytotoxicity against HepG2, MCF-7 and Caco-2 with IC_{50} 8.3 ±0.004, 9.1 ±0.03 and 11.4 ±0.004 $\mu g.mL^{-1}$, respectively. However, the extracts E1, E2, J7 and J9 were inactive.

Structural elucidation of the isolated compounds.

Six compounds (**Fig. 2**) were identified by the spectroscopic data analysis and comparison with literature data values (supplementary data). They were identified as triolein (**1**) (Cantrell et al.,

2011; Kumar et al., 2011; Thoss et al., 2012), oleic acid (**2**) (Sacchi et al., 1997), beta-sitosterol (**3**) (Ododo et al., 2016), methyl oleate (**4**) (Wineburg and Swern, 1972), butyrolactone-I (**5**) (Rao et al., 2000; Nagia et al., 2012; da Silva et al., 2017) and aspulvinone E (**6**) (Sugiyama et al., 1979; Gao et al., 2013)**.**

Docking analysis

In a critical trial to gain insight into the possible mechanisms at which these compounds exert their anticancer activity, the compounds were docked into various active sites, such as PIM, EGFR, VEGFR, FLT3, CDK2, CDK9, FAK, P53 and tubulin. The selection of the most promising poses was based on the interaction energies of the compounds within the various receptors and the binding interactions within the key residues inside the active sites. The obtained docking analyses revealed that only aspulvinone E (**6**) showed favorable binding affinity to FLT3 and EGFR active sites, whereas butyrolactone-I (**5**) revealed a strong interaction within the CDK2 active site. Conversely, no other compounds revealed acceptable results within the abovementioned proteins.

***In vitro* enzyme inhibitory assay**

Based on the abovementioned docking results, the active docked cytotoxic compounds, Butyrolactone-I (**5**) and aspulvinone E (**6**), were chosen to evaluate their *in vitro* enzymatic inhibitory activities. Butyrolactone-I (**5**) was assessed against Cdk2/A2 protein kinase, while aspulvinone E (**6**) assessed utilizing the kinase assay against both EGFR and FLT3 enzymes as presented in **Table 2**, the results were expressed as an IC_{50} (µM) value.

***In vitro* cytotoxic activities of Butyrolactone-I (5) and aspulvinone E (6)**

The pure isolated compounds, Butyrolactone-I (**5**) and Aspulvinone E (**6**), were evaluated for their cytotoxic activities against the cancer cell lines HepG2, MCF-7, and Caco-2 cancer cell lines. The

results were presented in Table 3. According to the findings, Butyrolactone-I (**5**) demonstrated cell proliferation inhibitory activity towards hepatocarcinoma (HepG2), and colorectal adenocarcinoma (Caco-2) with IC_{50} values of 17.83 ±0.32 and 25.93 ±0.48 µM, respectively, and weak antiproliferative activity against mammary gland breast cancer (MCF-7) cell line with IC_{50} value of 62.88 ±0.98 µM, in comparison to the reference drug Staurosporine. However, aspulvinone E (**6**) displayed weak cytotoxicity against HepG2 cell line (IC_{50} value= 78.5 ±0.97 µM), and no cytotoxicity against MCF-7 and Caco-2 (IC_{50} >100 µM) as shown in **Table 3**.

Discussion

Researchers and experts are still puzzled by the serious disease called cancer; finding cytotoxic medications that improve patient outcomes has always attracted scientist's interest. On the other hand, a recent review of endophytic *Aspergillus* species (El-hawary et al., 2020) showed that this endophytic strain is a rich source of chemicals with biological potential, including butenolides, alkaloids, sterols, and terpenoids. These reasons are what spur us to keep looking into cytotoxic metabolites in such a promising strain. The current study demonstrated the cytotoxic abilities of various extracts obtained from the OSMAC technique against the cancer cell lines, human hepatoma (HepG-2), human breast adenocarcinoma (MCF-7), and human colon adenocarcinoma (Caco-2). Cytotoxic study revealed that the fungal mycelia extract derived from the fermentation of isolated strain on MPDB media (J4) showed the best cytotoxic activity against the tested cancer cell lines, HepG-2, MCF-7 and Caco-2 with IC_{50} values of 4.2 ±0.13, 5.9 ±0.013 and 7.3 ±0.004 µg/mL, respectively. MPDB media extract (J4) was scaled up and subjected to further chromatographic investigation in order to explore its major chemical constituents and obtain promising cytotoxic compounds. Chromatographic study resulted in the isolation of six compounds including three fatty acids identified as, three fatty acids (**1, 2** and **4**), one sterol (**3**),

and two butenolides (**5** and **6**). Triolein (**1**) is a triglyceryl ester of monounsaturated fatty acid, that was previously reported in the seed oil of the indian folk remedy, *Jatropha curcas* L. (Cantrell et al., 2011) and in Bluebell seeds (Thoss et al., 2012). Oleic acid (**2**) is a monounsaturated fatty acid, and is one of the essential fatty acids that is abundent in olive oil (Sacchi et al., 1997). β-sitosterol (**3**) is a phytosterol that is primarily isolated from medicinal plants. However, recent studies demonstrated the isolation of β-sitosterol from endophytic fungal sources, *viz*, carvalho et. al. reported the isolation of β-sitosterol from the endophytic fungus *Colletotrichum gloeosporioides* hosted in the plant *Virola michelli* (Carvalho et al., 2016). It was also isolated from the endophytic fungus *Aspergillus niger* subsp. taxi HD86-9 associated with *Taxus cuspidata* Sieb. (Li et al., 2017), and from the soil fungus *Aspergillus* sp. FRIZ12 (Pinheiro et al., 2018), as well as, from the endophytic fungus *Aspergillus* N830 derived from the stems of *Gleditsia caspia* Desf. (Hagag et al., 2022). Methyl oleate (**4**) is a methyl ester of monounsaturated fatty acid (Wineburg and Swern, 1972). Butyrolactone I (**5**) and aspulvinone E (**6**) belong to the chemical class butenolides, also known as Ɣ-butyrolactones. Butenolides are class of fungal secondary metabolites that were previously isolated from various *Aspergillus* species. Butenolides are composed of a five-membered lactone bearing two aromatic rings. They exhibit a wide range of biological activities (Ibrahim et al., 2017). Butyrolactone I (**5**) is a butenolide obtained mostly from *A. terreus* that was initially isolated in 1977 from *A. terreus* (da Silva et al., 2017). It was reported from the endophytic fungus *Aspergillus terreus* isolated from the leaves of *Camellia sinensis* (Guo et al., 2016), and from *Aspergillus terreus* associated with *Hyptis suaveolens* (L.) Poit (da Silva et al., 2017) and *Suriana maritima* L. (Liao et al., 2018), also produced by the endophyte *Aspergillus versicolor* obtained from the roots of *Pulicaria crispa* (Ibrahim et al., 2016; Mohamed et al., 2020). Aspulvinones are yellow pigments made by fungi belonging to the *Aspergillus* family that include

a phenyl group at C-3 and benzyl groups at C-5 attached to a butenolide unit. In 1973, *Aspergillus terreus* was the first to report this class of natural compounds (Sugiyama et al., 1979). Aspulvinone E (**6**) was earlier isolated from *Aspergillus terreus* (Golding, et al., 1975; Gao *et al.*, 2013) and *Aspergillus flavipes* (Nagia et al., 2012).

The isolated compounds were subjected to further studies, including *in-silico* docking analysis against various cancer active sites, and *in vitro* enzyme assay in order to validate their cytotoxic potential.

Docking analysis

The application of molecular docking technology is a crucial step in scientific research since it offers a powerful computational filter that can be used to cut down on the time and money needed for effective drug development while also providing a clear understanding of the bioactive mechanisms (El-Hawary et al., 2022). Herein, docking study was carried out for the isolated compounds against various active sites, which nominated the two butenolides, butyrolactone-I (**5**) and aspulvinone E **(6)** as potential cytotoxic compounds based on their interaction energies within the various receptors and binding interactions within the key residues inside the active sites compared to the co-crystallized ligand.

The binding mode of butyrolactone-I (**5**) revealed substantial binding interactions within CDK2 active site and was approximately the same as the native ligand AZD5438, with a binding score of -7.49 and -8.79 Kcal/mol, respectively (PDB ID: 6GUH) (Wood et al., 2019). The 5-oxo-2,5-dihydrofuran-2-carboxylate formed two hydrogen bonds with the key residues Lys33 and Asn132 at 3.01 and 3.27 Å, respectively (**Figure 3A**). The 4-hydroxyphenyl-dihydrofuran moiety of **5** pointed to the gatekeeper residue Phe80, and its hydroxyl group formed a hydrogen bond with the

key amino acid Lys83 at 2.78 Å. Unlike the native ligand, the presence of the phenolic moiety at C3 of the dihydrofuran ring compensated additional interaction within the CDK2 active site (π-H interaction with Gly13 amino acid at 3.58 Å) (**Figure 3B**). On the other hand, the methylbutyl-2-ene of **5** did not allow the essential binding with Lys89. Because of this reason, it might be best to further modify methylbutyl-2-ene moiety with a hydrogen bond acceptor.

Aspulvinone E **(6)** demonstrated strong binding affinity, among the screened compounds, to FLT3 active site (PDB ID: 6JQR) (Kawase et al., 2019). **Figure 4A** revealed that the furan ring's carbonyl oxygen binds within the FLT3 active site via a hydrogen bond with the key amino acid residue Cys694 at 3.31 Å (the same as the native ligand gilteritinib). The phenolic hydroxyl group of **6** formed single hydrogen bonds with Cys695 at 3.07 Å. Besides, aspulvinone E (**6)** showed several π-H interactions with Leu616, Val624, and Phe691 amino acids. Despite these interesting interactions, compound **6** did not show the same binding affinity as gilteritinib (-6.86 and -8.48 kcal/mol, respectively). This might be because gilteritinib bears 4-amino-tetrahydropyrane moiety which occupies the hydrophobic lower part in the FLT3 active site, whereas **6** lacks this essential moiety (**Figure 4B**). Hence, adding a hydrophobic moiety attached to the 4-hydroxyfuran would further improve the affinity within FLT3 active site.

Analyzing the X-ray structure of EGFR (PDB ID: 2RGP), it was found that the native co-crystallized inhibitor of EGFR got stabilized inside the binding pocket through the formation of two H-bonds with Met793 amino acid (Xu et al., 2008). This indicates the great importance of Met793 binding for producing the EGFR antagonistic effect. On the other hand, the docked co-crystallized inhibitor of EGFR (HYZ) achieved a binding score of -11.33 Kcal/mol. It formed two H-bonds with Met793 amino acid at 3.13 and 3.19 Å, besides, one π-H bond with Lys745 amino acid at 4.13 Å (**Figure 4C**). However, **6** was observed to be able to bind the crucial amino acid

Met397 with one hydrogen bond at 3.02 Å. Besides, it formed one hydrogen bond with Ser720 at 3.35 Å, and three π-H bonds with Leu718, Phe723, and Val726 amino acid. Its binding score was found to be -7.01 Kcal/mol. Despite the different orientation of **6** and the native ligand within the EGFR active site, **6** nearly occupied the pocket and interacted with the key amino acid residue Met397 (**Figure 4D**). Additionally, adding an extension to 4-hydroxyfuran moiety of **6** could result in more EGFR active site occupying. Interestingly, the superimposition of **6** with gilteritinib and HYZ (the native ligands in FLT3 and EGFR active sites) showed the importance of further optimizing **6** by adding a hydrophobic extension to the 4-hydroxyfuran moiety. Based on the above, we can conclude the expected affinity and the corresponding intrinsic activity of **6** as a potential FLT3/EGFR inhibitor.

The *in-silico* docking findings were supplemented by the *in vitro* enzyme inhibitiory testing results which confirmed the observed results.

In vitro Cdk2/A2 inhibition assay

Cdk2 participates in a variety of important cellular activities upon binding with its activating proteins, cyclin E or A. Its interaction with cyclin A allows for continued DNA replication and well-controlled E2F inactivation. Cancer, Alzheimer's, Parkinson's, stroke, diabetes, polycystic kidney disease, glomerulonephritis, inflammation, and AIDS are just a few of the illnesses that Cdks play a role in (Niu et al., 2008). Besides, many studies revealed that CDK2 is overexpressed in various malignancies, such as melanoma, ovarian, pancreatic and lung carcinoma. Moreover, current investigations support Cdk2's potential as an anticancer therapeutic target (Abd El-Karim et al., 2019). Thus, the Cdk2/A2 inhibitory activity of compound **5** was studied *in-vitro*. Butyrolactone-I (**5**) showed significant inhibitory activity against the target enzyme Cdk2/A2 twice that of the reference compound roscovitine (IC_{50} = 0.747 ± 0.017 *vs.* 1.680 ± 0.031 µM).

In vitro EGFR and FLT3 inhibition assay

The epidermal growth factor receptor (EGFR) signaling system has been widely studied for it's role in the advancement of several types of malignant tumors. On the other hand, the development of small molecules that target EGFR is a well-known technique for anticancer drug development (Allam et al., 2020). EGFR and FLT3 inhibitory activity of aspulvinone E (**6**) was evaluated. The obtained results revealed that aspulvinone E (**6**) is a promising EGFR inhibiting candidate (IC_{50} = 0.459 ± 0.008 µM) compared to the reference drug lapatinib (IC_{50} = 0.074 ± 0.003 µM). It also exhibited FLT3 inhibitory activity with IC_{50} value of 0.841 ± 0.011 µM compared to the standard control drug sorafenib (IC_{50} = 0.178 ± 0.004 µM).

According to the aforementioned enzyme inhibitory results, the isolated butenolide derivatives, butyrolactone-I (**5**) and aspulvinone E (**6**), demonstrated strong enzyme inhibitory activities and promising cytotoxic potential. They were therefore tested for their cytotoxic effect against the three cancer cell lines, HepG2, MCF-7, and Caco-2 *in vitro* using MTT assay. Compared to the common cytotoxic drug (Staurosporine), butyrolactone-I (**5**) exhibited cytotoxic efficacy against HepG2 and Caco-2 cell lines (IC_{50} values of 17.83 ±0.32 and 25.96 ±0.48 µM, respectively). Thus, our findings showed that butyrolactone-I (**5**) might be employed to prevent the growth of cancerous HepG-2 and Caco-2 cells by inhibiting Cdk2 enzyme activity. However, despite butyrolactone-I (**5**) being a powerful Cdk2 inhibitor, only mildly affected MCF-7 cancer cell line (IC_{50} value= 62.94 ±0.98 µM). This is due to the fact that Cdk2 is so poorly expressed in MCF-7 cells, and not the main factor influencing the prognosis of breast cancer (Comşa et al., 2015). On the other hand, aspulvinone E (**6**) displayed weak cytotoxicity against HepG-2 cell line (IC_{50} value= 78.5 ±0.97 µM), and no cytotoxicity against MCF-7 and Caco-2 with IC_{50} values >100 µM, although its potent enzyme inhibitory activity against EGFR and FLT3, which motivated us to look into this point;

studies revealed that the epidermal growth factor receptor (EGFR) is a robust prognostic indicator in the five cancers, ovarian, bladder, cervical, oesophageal, head and neck cancers, and a weak prognostic indicator in breast cancer (Nicholson et al., 200; Comşa et al., 2015). While, FLT3 is greatly overexpressed in human leukemia-lymphoma cell lines (DaSilva et al., 1994; Drexler, 1996). Therefore, the investigated cancer cell lines (MCF-7, HepG2, and Caco-2) exhibit low levels of EGFR and FLT3 enzyme expression, which justifies the low cytotoxicity of aspulvinone E (**6**) towards these cell lines, and supports the hypothesis that aspulvinone E (**6**) has an affinity for these two receptors. We thus recommend further investigation into aspulvinone E (**6**) as a promising anti-EGFR and anti-FLT3 medication for the treatment of cancers that are significantly affected by these enzymes.

Cytotoxic background of butyrolactone I (5) and aspulvinone E (6)

According to previous studies, butyrolactone-I showed mild cytotoxic activity against MCF-7/ADR (human breast cancer), U251 (human CNS cancer), SW620 (human colon cancer), DU145 (human prostate cancer), and A498 (human renal cancer) (Rao et al., 2000). In addition, it inhibited cell proliferation in L-929 (mouse fibroblasts) and K562 (human chronic myeloid leukemia) cell lines with GI_{50} values of 32.3 and 20.2 µM, respectively. It also demonstrated cytotoxicity against HeLa (human cervix carcinoma) cells, with a CC_{50} value of 66.3 µM (Niu et al., 2008). Butyrolactone-I showed weak cytotoxicity against HL-60 (Caucasian promyelocytic leukemia) with an IC_{50} value of 57.5 µM (Wang et al., 2011). Haritakun et al., revealed that butyrolactone-I exhibited weak cytotoxicity towards KB (oral epidermoid carcinoma), MCF-7 (breast cancer), NCI-H187 (small-cell lung cancer), and noncancerous *Vero* cells (African green monkey kidney fibroblasts) (Haritakun et al., 2010). Additionally, Ma et al. reported that butyrolactone-I demonstrated either very weak or undetectable cytotoxicity (IC_{50} > 50 µM) against P388 (Mouse

lymphoid macrophage), K562 (chronic myelogenous leukemia), A-549 (human lung adenocarcinoma epithelial cell line) and HeLa cell lines (Ma et al., 2014). A recent study showed that butyrolactone-I demonstrated potent cytotoxicity towards ovarian adenocarcinoma cells (SKOV3) (IC_{50} 0.6 µg.mL^{-1}), and metastatic prostate cells (PC-3) (IC_{50} 4.5 µg/mL) (Ghfar et al., 2021). On the other hand, different studies revealed that butyrolactone-I **(5)** is a naturally occurring cyclin-dependent kinase (CDK) inhibitor, thus it has a potential therapeutic effect, particularly as inhibitor of cancer cell growth. Suzuki et al., demonstrated that butyrolactone-I specifically inhibited cyclin-dependent kinase B1 in the three human prostate cancer cell lines (DU145, PC-3, and LNCaP), while other cyclins (D2 and A) were not significantly affected (Suzuki et al., 1999). Furthermore, butyrolactone-I discriminated among members of the Cdk inhibitors family as it inhibited cell cycle kinases, cdc2, cdk1, cdk2, cdk5/p25, cdk5, cdk1/cyclin B, cdc2/cyclin B and cdk2/cyclin A, selectively, and increases in Cx43 phosphorylation *in vitro* and *in vivo* during mitosis (Kitagawa et al., 1994; Kanemitsu et al., 1998; Fischer and Lane, 2000; Niu et al., 2008). It also inhibited PKC, PKA, MAPK PKA, CK II PKA, CK I PKA, and Tyr with IC_{50} values of 0.6, 1.5, 160, 260, 94, 240, 590, and 590 µM, respectively. On the other hand, despite the fact that aspulvinone E is a highly valued compound and demonstrated a numerous therapeutic effects, such as antibacterial (Nagia et al., 2012), antiviral (Gao et al., 2013; El-Hawary et al., 2021) and anti-HIV (Pang et al., 2017), there are insufficient research studies regarding its cytotoxic actions. Only one study in 2013 by Gao et al., declared that aspulvinone E showed no cytotoxic activity against A549 and MDCK (Madin-Darby canine kidney) cell lines (CC_{50} >250 µg/mL) (Gao et al., 2013). Furthermore, Aspulvinone E has never been reported to inhibit protein kinases or tyrosine kinases. As a result, this is the first report on the activity of aspulvinone E (**6**) as a tyrosine kinase inhibitor, particulary against FLT3 and EGFR.

Acknowledgment

We thank NUB for providing laboratory space.

Confict of Interest

None declared

Availability of data and materials

All data generated or analyzed during this study are included in this published article (and its supplementary information fles).

References

Abd El-Karim, S.S., Syam, Y.M., El Kerdawy, A.M., Abdelghany, T.M., 2019. New thiazol-hydrazono-coumarin hybrids targeting human cervical cancer cells: Synthesis, CDK2 inhibition, QSAR and molecular docking studies. Bioorg. Chem. 86, 80–96. https://doi.org/10.1016/j.bioorg.2019.01.026

Abdelaleem, E.R., Samy, M.N., Ahmed, S.A., Aboulmagd, A.M., Alhadrami, A.H., Rateb, M.E., Abdelmohsen, U.R., Desoukey, S.Y., 2022. The Red Sea marine sponge Spongia irregularis: metabolomic profiling and cytotoxic potential supported by in silico studies. Nat. Prod. Res. 1–5.

Ahmed, S.S.T., Fahim, J.R., Youssif, K.A., Amin, M.N., Abdel-Aziz, H.M.H., Brachmann, A.O., Piel, J., Abdelmohsen, U.R., Hamed, A.E., 2021. Cytotoxic potential of Allium sativum L . roots and their green synthesized nanoparticles supported with metabolomics and molecular docking analyses. South African J. Bot. 142, 131–139. https://doi.org/10.1016/j.sajb.2021.06.020

548 Allam, H.A., Aly, E.E., Farouk, A.K.B.A.W., El Kerdawy, A.M., Rashwan, E., Abbass, S.E.S.,
549 2020. Design and Synthesis of some new 2,4,6-trisubstituted quinazoline EGFR inhibitors as
550 targeted anticancer agents. Bioorg. Chem. 98, 103726.
551 https://doi.org/10.1016/j.bioorg.2020.103726

552 Cantrell, C.L., Ali, A., Duke, S.O., Khan, I., 2011. Identification of mosquito biting deterrent
553 constituents from the indian folk remedy plant Jatropha curcas. J. Med. Entomol. 48, 836–
554 845. https://doi.org/10.1603/ME10244

555 Carvalho, J.M., da Paixão, L.K.O., Dolabela, M.F., Marinho, P.S.B., Marinho, A.M.D.R., 2016.
556 Phytosterols isolated from endophytic fungus Colletotrichum gloeosporioides
557 (Melanconiaceae). Acta Amaz. 46, 69–72. https://doi.org/10.1590/1809-4392201500072

558 Comşa, Ş., Cîmpean, A.M., Raica, M., 2015. The story of MCF-7 breast cancer cell line: 40 Years
559 of experience in research. Anticancer Res. 35, 3147–3154.

560 da Silva, I.P., Brissow, E., Claudio, L., Filho, K., Senabio, J., Crispim, D., Lizandra, T.,
561 Magalhães, G., Ademar, P., Junior, S., Helena, A., Soares, M.A., 2017. Bioactive compounds
562 of Aspergillus terreus — F7 , an endophytic fungus from Hyptis suaveolens (L .) Poit. World
563 J. Microbiol. Biotechnol. 33, 62. https://doi.org/10.1007/s11274-017-2228-3

564 DaSilva, N., Hu, Z.B., Ma, W., Rosnet, O., Birnbaum, D., Drexler, H.G., 1994. Expression of the
565 FLT3 gene in human leukemia-lymphoma cell lines. Leukemia 8, 885–888.

566 Drexler, H.G., 1996. Expression of FLT3 receptor and response to FLT3 ligand by leukemic cells.
567 Leukemia 10, 588–599.

568 El-hawary, S.S., Moawad, A.S., Bahr, H.S., Abdelmohsen, U.R., Mohammed, R., 2020. Natural

product diversity from the endophytic fungi of the genus Aspergillus. RSC Adv. 10, 22058–22079. https://doi.org/10.1039/d0ra04290k

El-Hawary, S.S., Mohammed, R., Bahr, H.S., Attia, E.Z., El-Katatny, M.H., Abelyan, N., Al-Sanea, M.M., Moawad, A.S., Abdelmohsen, U.R., 2021. Soybean-associated endophytic fungi as potential source for anti-COVID-19 metabolites supported by docking analysis. J. Appl. Microbiol. 131, 1193–1211. https://doi.org/10.1111/jam.15031

El-Hawary, S.S., Mohammed, R., Bahr, H.S., Attia, E.Z., El-Katatny, M.H., Abelyan, N., Al-Sanea, M.M., Moawad, A.S., Abdelmohsen, U.R., 2021. Soybean-associated endophytic fungi as potential source for anti-COVID-19 metabolites supported by docking analysis. J. Appl. Microbiol. 131, 1193–1211. https://doi.org/10.1111/jam.15031

El-Hawary, S.S., Mohammed, R., Taher, M.A., Abouzid, S.F., Mansour, M.A., Almahmoud, S.A., Huwaimel, B., Amin, E., 2022. Characterization of Promising Cytotoxic Metabolites from Tabebuia guayacan Hemsl.: Computational Prediction and *In vitro* Testing. Plants 11. https://doi.org/10.3390/plants11070888

El-Hawary, Seham S., Mohammed, R., Tawfike, A.F., Lithy, N.M., Abouzid, S.F., Amin, M.N., Abdelmohsen, U.R., Amin, E., 2021. Cytotoxic activity and metabolic profiling of fifteen euphorbia species. Metabolites 11, 1–18. https://doi.org/10.3390/metabo11010015

Elebeedy, D., Badawy, I., Elmaaty, A.A., Saleh, M.M., Kandeil, A., Ghanem, A., Kutkat, O., Alnajjar, R., Abd El Maksoud, A.I., Al-Karmalawy, A.A., 2022. *In vitro* and computational insights revealing the potential inhibitory effect of Tanshinone IIA against influenza A virus. Comput. Biol. Med. 141, 105149.

Elebeedy, D., Elkhatib, W.F., Kandeil, A., Ghanem, A., Kutkat, O., Alnajjar, R., Saleh, M.A., Abd

El Maksoud, A.I., Badawy, I., Al-Karmalawy, A.A., 2021. Anti-SARS-CoV-2 activities of tanshinone IIA, carnosic acid, rosmarinic acid, salvianolic acid, baicalein, and glycyrrhetinic acid between computational and *in vitro* insights. RSC Adv. 11, 29267–29286. https://doi.org/10.1039/D1RA05268C

Elkhayat, E.S., Ibrahim, S.R.M., Mohamed, G.A., Ross, S.A., 2015. Terrenolide S , a new antileishmanial butenolide from the endophytic fungus Aspergillus terreus. Nat. Prod. Res. 30, 814–820. https://doi.org/10.1080/14786419.2015.1072711

Elmaaty, A.A., Darwish, K.M., Chrouda, A., Boseila, A.A., Tantawy, M.A., Elhady, S.S., Shaik, A.B., Mustafa, M., Al-Karmalawy, A.A., 2022. In Silico and *in vitro* Studies for Benzimidazole Anthelmintics Repurposing as VEGFR-2 Antagonists: Novel Mebendazole-Loaded Mixed Micelles with Enhanced Dissolution and Anticancer Activity. ACS Omega 7, 875–899. https://doi.org/10.1021/acsomega.1c05519

Elmaidomy, A.H., Mohammed, R., Hassan, H.M., Owis, A.I., Rateb, M.E., Khanfar, M.A., Krischke, M., Mueller, M.J., Abdelmohsen, U.R., 2019. Metabolomic profiling and cytotoxic tetrahydrofurofuran lignans investigations from Premna odorata Blanco. Metabolites 9, 223. https://doi.org/10.3390/metabo9100223

Farouk, H.M., Attia, E.Z., El-katatny, M.H., 2020. Hydrolytic enzyme production of endophytic fungi isolated from soybean (Glycine max). J. Mod. Res. 2, 1–7.

Fischer, P.M., Lane, D.P., 2000. Inhibitors of cyclin-dependent kinases as cancer therapeutics. Curr. Med. Chem. 7, 1213–1245. https://doi.org/10.1016/j.pharmthera.2017.02.008

Gao, H., Guo, W., Wang, Q., Zhang, L., Zhu, M., Zhu, T., Gu, Q., Wang, W., Li, D., 2013. Aspulvinones from a mangrove rhizosphere soil-derived fungus Aspergillus terreus Gwq-48

with anti-influenza A viral (H1N1) activity. Bioorganic Med. Chem. Lett. 23, 1776–1778. https://doi.org/10.1016/j.bmcl.2013.01.051

Gary Gilliland, D., Griffin, J.D., 2002. The roles of FLT3 in hematopoiesis and leukemia. Blood 100, 1532–1542. https://doi.org/10.1182/blood-2002-02-0492

Ghfar, A.A., El-metwally, M.M., Shaaban, M., Gabr, S.A., Gabr, N.S., Diab, M.S.M., Aqel, A., Habila, M.A., Al-qahtani, W.H., Alfaifi, M.Y., Elbehairi, S.E.I., Aljumah, B.A., 2021. Thermophilic Aspergillus terreus TM8 Promoted Apoptosis and. Molecules 26, 1–8.

Golding, B.T., Rickards, R.W., Vanek, Z., 1975. New Metabolites of Aspergillus terreus : 3-Hydroxy-2,5- bis-(p- hydroxy- phenyl) penta-2,4-d ien-4-olide and Derivatives. Chem. Soc. Perkin Trans I 19, 1961–1963.

Guo, F., Li, Z., Xu, X., Wang, K., Shao, M., Zhao, F., Wang, H., Hua, H., Pei, Y., Bai, J., 2016. Butenolide derivatives from the plant endophytic fungus Aspergillus terreus. Fitoterapia 113, 44–50. https://doi.org/10.1016/j.fitote.2016.06.014

Hagag, A., Abdelwahab, M.F., Abd El-kader, A.M., Fouad, M.A., 2022. The endophytic Aspergillus strains: A bountiful source of natural products. J. Appl. Microbiol. 132, 4150–4169. https://doi.org/10.1111/jam.15489

Haluska, P., Adjei, A.A., 2001. Receptor tyrosine kinase inhibitors. Curr. Opin. Investig. Drugs (London, Engl. 2000) 2, 280–286.

Haritakun, R., Rachtawee, P., Chanthaket, R., Boonyuen, N., Isaka, M., 2010. Butyrolactones from the Fungus Aspergillus terreus BCC 4651. Chem. Pharm. Bull. 58, 1545–1548.

Ibrahim, S.R.M., Mohamed, G.A., Ross, S.A., 2017. Aspernolides L and M , new butyrolactones

from the endophytic fungus Aspergillus versicolor. Z. Naturforsch 72, 155–160. https://doi.org/10.1515/znc-2016-0138

Kanemitsu, M.Y., Jiang, W., Eckhart, W., 1998. Cdc2-mediated phosphorylation of the gap junction protein, connexin43, during mitosis. Cell growth Differ. Mol. Biol. J. Am. Assoc. Cancer Res. 9, 13–21.

Kawase, T., Nakazawa, T., Eguchi, T., Tsuzuki, H., Ueno, Y., Amano, Y., Suzuki, T., Mori, M., Yoshida, T., 2019. Effect of Fms-like tyrosine kinase 3 (FLT3) ligand (FL) on antitumor activity of gilteritinib, a FLT3 inhibitor, in mice xenografted with FL-overexpressing cells. Oncotarget 10, 6111.

Kharwar, R.N., Mishra, A., Gond, S.K., Stierle, D., 2011. Anticancer compounds derived from fungal endophytes : their importance and future challenges. Nat. Prod. Rep. 28, 1208–1228. https://doi.org/10.1039/c1np00008j

Khattab, M., Al-Karmalawy, A.A., 2021. Computational repurposing of benzimidazole anthelmintic drugs as potential colchicine binding site inhibitors. Future Med. Chem. 13, 1623–1638.

Kitagawa, M., Higashi, H., Takahashi, I.S., Okabe, T., Ogino, H., Taya, Y., Hishimura, S., Okuyama, A., 1994. A cyclin-dependent kinase inhibitor, butyrolactone I, inhibits phosphorylation of RB protein and cell cycle progression. Oncogene 9, 2549–2557.

Kumar, R., Bansal, V., Tiwari, A.K., Sharma, M., Puri, S.K., Patel, M.B., Sarpal, A.S., 2011. Estimation of glycerides and free fatty acid in oils extracted from various seeds from the Indian region by NMR spectroscopy. J. Am. Oil Chem. Soc. 88, 1675–1685. https://doi.org/10.1007/s11746-011-1846-4

Lees, E., 1995. Cyclin dependent kinase regulation. Curr. Opin. Cell Biol. 7, 773–780. https://doi.org/10.1016/0955-0674(95)80060-3

Li, D., Fu, D., Zhang, Y., Ma, X., Gao, L., Wang, X., Zhou, D., Zhao, K., 2017. Isolation, purification, and identification of taxol and related taxanes from taxol-producing fungus Aspergillus niger subsp. Taxi. J. Microbiol. Biotechnol. 27, 1379–1385. https://doi.org/10.4014/jmb.1701.01018

Liao, G., Wu, P., Xue, J., Liu, L., Li, H., Wei, X., 2018. Asperimides A – D , anti-in fl ammatory aromatic butenolides from a tropical endophytic fungus Aspergillus terreus. Fitoterapia 131, 50–54. https://doi.org/10.1016/j.fitote.2018.10.011

Ma, X., Zhu, T., Gu, Q., Xi, R., Wang, W., Li, D., 2014. Structures and antiviral activities of butyrolactone derivatives isolated from Aspergillus terreus MXH-23. J. Ocean Univ. China 13, 1067–1070. https://doi.org/10.1007/s11802-014-2324-z

Mahmoud, A., Mostafa, A., Al-Karmalawy, A.A., Zidan, A., Abulkhair, H.S., Mahmoud, S.H., Shehata, M., Elhefnawi, M.M., Ali, M.A., 2021. Telaprevir is a potential drug for repurposing against SARS-CoV-2: computational and *in vitro* studies. Heliyon 7, e07962. https://doi.org/10.1016/J.HELIYON.2021.E07962

Mahmoud, D.B., Bakr, M.M., Al-Karmalawy, A.A., Moatasim, Y., El Taweel, A., Mostafa, A., 2022. Scrutinizing the Feasibility of Nonionic Surfactants to Form Isotropic Bicelles of Curcumin: a Potential Antiviral Candidate Against COVID-19. AAPS PharmSciTech 23, 1–12.

Mohamed, G.A., Ibrahim, S.R.M., Asfour, H.Z., 2020. Antimicrobial metabolites from the endophytic fungus Aspergillus versicolor. Phytochem. Lett. 35, 152–155.

678 Nagia, M.M., El-Metwally, M.M., Shaaban, M., El-Zalabani, S.M., Hanna, A.G., 2012. Four
679 butyrolactones and diverse bioactive secondary metabolites from terrestrial Aspergillus
680 flavipes MM2: isolation and structure determination. Org. Med. Chem. Lett. 2, 1–8.
681 https://doi.org/10.1186/2191-2858-2-9

682 Nicholson, R.I., Gee, J.M.W., Harper, M.E., 2001. EGFR and cancer prognosis. Eur. J. Cancer 37,
683 9–15. https://doi.org/10.1016/s0959-8049(01)00231-3

684 Niu, X., Dahse, H.M., Menzel, K.D., Lozach, O., Walther, G., Meijer, L., Grabley, S., Sattler, I.,
685 2008. Butyrolactone I derivatives from Aspergillus terreus carrying an unusual sulfate
686 moiety. J. Nat. Prod. 71, 689–692. https://doi.org/10.1021/np070341r

687 Ododo, M.M., Choudhury, M.K., Dekebo, A.H., 2016. Structure elucidation of β-sitosterol with
688 antibacterial activity from the root bark of Malva parviflora. Springerplus 5, 2–11.
689 https://doi.org/10.1186/s40064-016-2894-x

690 Orfali, R., Aboseada, M.A., Abdel-Wahab, N.M., Hassan, H.M., Perveen, S., Ameen, F., Alturki,
691 E., Abdelmohsen, U.R., 2021. Recent updates on the bioactive compounds of the marine-
692 derived genusAspergillus, RSC Advances. Royal Society of Chemistry.
693 https://doi.org/10.1039/d1ra01359a

694 Owis, A.I., El-Hawary, M.S., El Amir, D., Aly, O.M., Abdelmohsen, U.R., Kamel, M.S., 2020.
695 Molecular docking reveals the potential ofSalvadora persicaflavonoids to inhibit COVID-19
696 virus main protease. RSC Adv. 10, 19570–19575. https://doi.org/10.1039/d0ra03582c

697 Pang, X., Zhao, J., Fang, X., Zhang, T., Zhang, D., Liu, H., Su, J., Cen, S., Yu, L., 2017.
698 Metabolites from the Plant Endophytic Fungus Aspergillus sp. CPCC 400735 and Their Anti-
699 HIV Activities. J. Nat. Prod. 80, 2595–2601. https://doi.org/10.1021/acs.jnatprod.6b00878

Pinheiro, E.A.A., Pina, J.R.S., Paixão, L.K.O., Siqueira, J.E.S., Feitosa, A.O., Carvalho, J.M., Marinho, P.S.B., Marinho, A.M.R., 2018. Chemical Constituents and Antimicrobial Activity of Soil Fungus Aspergillus sp. FRIZ12. Rev. virtual Quim. 10.

Rao, K. V., Sadhukhan, A.K., Veerender, M., Ravikumar, V., Mohan, E.V.S., Dhanvantri, S.D., Sitaramkumar, M., Babu, J.M., Vyas, K., Reddy, G.O., 2000a. Butyrolactones from Aspergillus terreus. Chem. Pharm. Bull. 48, 559–562.

Rao, K. V., Sadhukhan, A.K., Veerender, M., Ravikumar, V., Mohan, E.V.S., Dhanvantri, S.D., Sitaramkumar, M., Moses Babu, J., Vyas, K., Om Reddy, G., 2000b. Butyrolactones from Aspergillus terreus. Chem. Pharm. Bull. 48, 559–562. https://doi.org/10.1248/cpb.48.559

Sacchi, R., Addeo, F., Paolillo, L., 1997. 1H and 13CNMR of Virgin Olive Oil. An Overview. Magn. Reson. Chem. 35, 133–145. https://doi.org/10.1021/ci00008a007

Sayed, A.M., Khattab, A.R., AboulMagd, A.M., Hassan, H.M., Rateb, M.E., Zaid, H., Abdelmohsen, U.R., 2020. Nature as a treasure trove of potential anti-SARS-CoV drug leads: a structural/mechanistic rationale. RSC Adv. 10, 19790–19802. https://doi.org/10.1039/d0ra04199h

Shady, N.H., Tawfike, A.F., Yahia, R., Mostafa, A., Brachmann, A.O., Piel, J., Abdelmohsen, U.R., Kamel, M.S., 2021. Cytotoxic activity of actinomycetes Nocardia sp . and Nocardiopsi s sp . associated with marine sponge Amphimedon sp . Nat. Prod. Res. 1–6. https://doi.org/10.1080/14786419.2021.1931865

Shoala, T., Al-Karmalawy, A.A., Germoush, M.O., ALshamrani, S.M., Abdein, M.A., Awad, N.S., 2021. Nanobiotechnological Approaches to Enhance Potato Resistance against Potato Leafroll Virus (PLRV) Using Glycyrrhizic Acid Ammonium Salt and Salicylic Acid

722 Nanoparticles. Horticulturae 7, 402.

723 Sugiyama, H., Ojima, N., Kobayashi, M., Senda, Y., Ishiyama, J., Seto, S., 1979. C-13 NMR
724 Spectra of Aspulvinones. Agric. Biol. Chem. 43, 403–404.
725 https://doi.org/10.1080/00021369.1979.10863463

726 Suzuki, M., Hosaka, Y., Matsushima, H., Goto, T., Kitamura, T., Kawabe, K., 1999. Butyrolactone
727 I induces cyclin B1 and causes G2 / M arrest and skipping of mitosis in human prostate cell
728 lines. Cancer Lett. 138, 121–130.

729 Thoss, V., Murphy, P.J., Marriott, R., Wilson, T., 2012. Triacylglycerol composition of British
730 bluebell (Hyacinthoides non-scripta) seed oil. RSC Adv. 2, 5314–5322.
731 https://doi.org/10.1039/c2ra20090b

732 Uzma, F., Mohan, C.D., Hashem, A., Konappa, N.M., Rangappa, S., Kamath, P. V., Singh, B.P.,
733 Mudili, V., Gupta, V.K., Siddaiah, C.N., Chowdappa, S., Alqarawi, A.A., Abd-Allah, E.F.,
734 2018. Endophytic fungi-alternative sources of cytotoxic compounds: A review. Front.
735 Pharmacol. 9, 1–37. https://doi.org/10.3389/fphar.2018.00309

736 Wang, Q., Yang, Y., Yang, X., Miao, C., Li, Y., Liu, S., Luo, N., Ding, Z., Zhao, L., 2018.
737 Phytochemistry Lovastatin analogues and other metabolites from soil-derived Aspergillus
738 terreus YIM PH30711. Phytochemistry 145, 146–152.
739 https://doi.org/10.1016/j.phytochem.2017.11.006

740 Wang, Y., Zheng, J., Liu, P., Wang, W., Zhu, W., 2011. Three new compounds from Aspergillus
741 terreus PT06-2 grown in a high salt medium. Mar. Drugs 9, 1368–1378.
742 https://doi.org/10.3390/md9081368

743 Wineburg, J.P., Swern, D., 1972. NMR Chemical Shift Reagents in Structural Determination of
744 Lipid Derivatives: I1. Methyl Petroselinate and Methyl Oleate 1. Jorurnal Am. oil Chem. Soc.
745 49, 267–273.

746 Wood, D.J., Korolchuk, S., Tatum, N.J., Wang, L.-Z., Endicott, J.A., Noble, M.E.M., Martin, M.P.,
747 2019. Differences in the conformational energy landscape of CDK1 and CDK2 suggest a
748 mechanism for achieving selective CDK inhibition. Cell Chem. Biol. 26, 121–130.

749 Xu, G., Abad, M.C., Connolly, P.J., Neeper, M.P., Struble, G.T., Springer, B.A., Emanuel, S.L.,
750 Pandey, N., Gruninger, R.H., Adams, M., 2008. 4-Amino-6-arylamino-pyrimidine-5-
751 carbaldehyde hydrazones as potent ErbB-2/EGFR dual kinase inhibitors. Bioorg. Med. Chem.
752 Lett. 18, 4615–4619.

753 Youssif, K.A., Elshamy, A.M., Rabeh, M.A., Gabr, N., Afifi, W.M., Salem, M.A., Albohy, A.,
754 Abdelmohsen, U.R., Haggag, E.G., 2020. Cytotoxic Potential of Green Synthesized Silver
755 Nanoparticles of Lampranthus coccineus Extracts, Metabolic Profiling and Molecular
756 Docking Study. ChemistrySelect 5, 12278–12286. https://doi.org/10.1002/slct.202002947

757 **Authors Contributions**

758 E.Z.A., M.H.E., U.R.A, S.E, R.M., A.S.M and H.S.B were involved in conceptualization. E.Z.A.,
759 M.H.E., N.A., J.Z. and M.M.A were involved in methodology. E.Z.A., M.H.E., U.R.A, S.E, R.M.
760 and A.S.M were involved in data curation. U.R.A and H.S.B. were involved in original draft
761 preparation. M.E.R. was involved in spectral analysis of the isolated compounds. A.S.M and H.S.B
762 involved in elucidation of the isolated compounds. M.M and A.A.A carried out docking analysis.
763 All authors were involved in writing, review and editing. All authors have read and agreed to the
764 published version of the manuscript.

765

766

767

768 **Tables**

769 **Table 1:** IC_{50} µg.mL^{-1} values of *Aspergillus terreus* extracts in different cancer cell lines.

Cell line Code	**IC_{50} (µg.mL^{-1}) HepG2**	**IC_{50} (µg.mL^{-1}) MCF-7**	**IC_{50} (µg.mL^{-1}) Caco-2**
E1	> 50	> 50	> 50
E2	> 50	> 50	> 50
E4	21.4±0.017	22.6±0.031	23.8±0.011
E5	8.3±0.004	9.1±0.03	11.4±0.004
E7	17.4±0.017	18.3±0.011	19.7±0.031
J3	5.6±0.15	6.8±0.09	8.4±0.06
J4	4.2±0.13	5.9±0.013	7.3±0.004
J6	19.5±0.08	21.6±0.76	23.3±0.05
J7	> 50	> 50	> 50
J9	> 50	> 50	> 50

770 * Very significant difference compared with the corresponding doxorubicin IC_{50} values ($P < 0.05$).

Table 2: Enzyme inhibitory activities of the active butenolides isolated from the fungal mycelia fermented in Modified Potato Dexrose Broth (MPDB).

	CDK2 IC_{50} (µM)	EGFR IC_{50} (µM)	FLT3 IC_{50} (µM)
Roscovitine	1.680 ± 0.031		
Butyrolactone-I (5)	0.747 ± 0.017[a]		
Lapatinib		0.074 ± 0.003	
Aspulvinone E (6)		0.459 ± 0.008[b]	
Sorafenib			0.178 ± 0.004
Aspulvinone E (6)			0.841 ± 0.011[c]

Data in the table represent mean ± standard deviation (SD) where; [a] significantly different from positive control (Roscovitine), [b] significantly different from positive control (Lapatinib), [c] significantly different from positive control (Sorafenib) at $p < 0.05$.

Table 3: *In vitro* cytotoxic activity of the active butenolides isolated from the fungal mycelia fermented in Modified Potato Dexrose Broth (MPDB).

Sample	Cytotoxicity IC_{50} (µM)		
	HepG2	**MCF-7**	**Caco2**
Butyrolactone-I (5)	17.83 ±0.32	62.88 ±0.98	25.93 ±0.48
Aspulvinone E (6)	78.5 ±0.97	171.12 ±1.86	147.19 ±1.89
Staurosporine	9.69 ±0.19	7.99 ±0.14	11.66 ±0.24

Data in the table represent mean ± standard deviation (SD). Samples are significantly different from positive control (Staurosporine) at $p < 0.05$.

799

800

801 **Figures ligand**

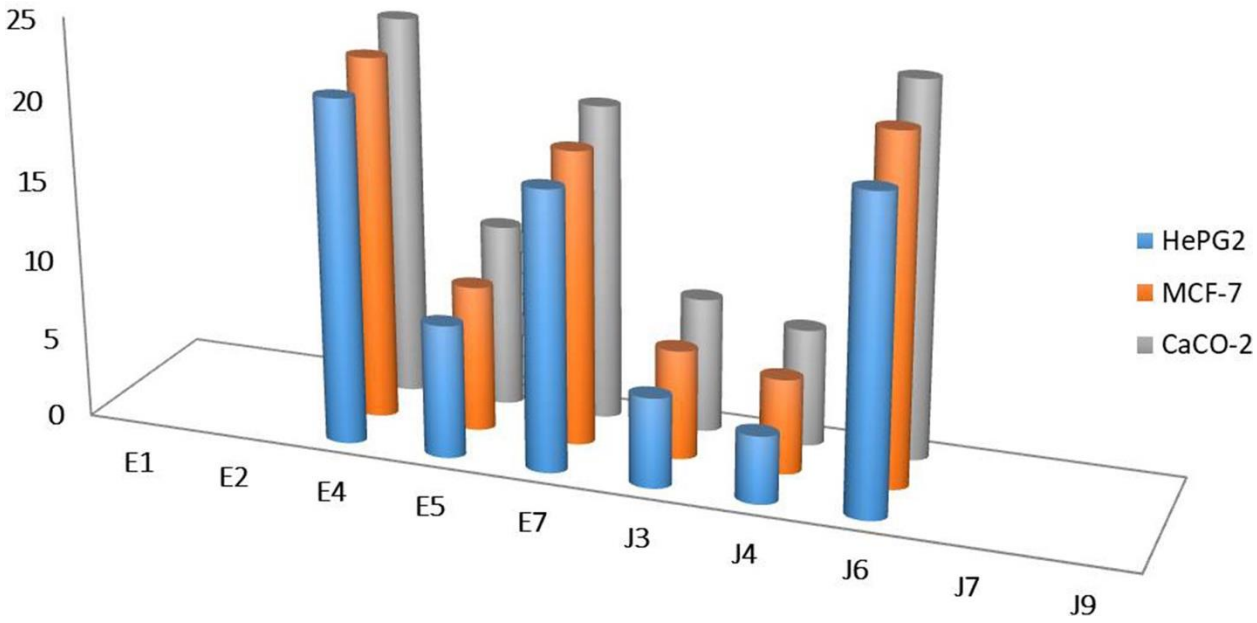

802

803 **Figure 1: IC_{50} µg.mL^{-1} values of *Aspergillus terreus* extracts in different cancer cell lines.**

804 Where, Potato dextrose broth culture extract (E1); Modified potato dextrose broth culture extract

805 (E2); Sabouraud Broth extract (E4); Malt Extract Broth (E5); Rice Extract Broth (E7); Potato

806 dextrose mycelia culture extract (J3); Modified potato dextrose mycelia culture extract (J4);

807 Sabouraud mycelia extract (J6); Malt culture broth mycelia extract (J7); Rice culture broth mycelia

808 extract (J9).

809

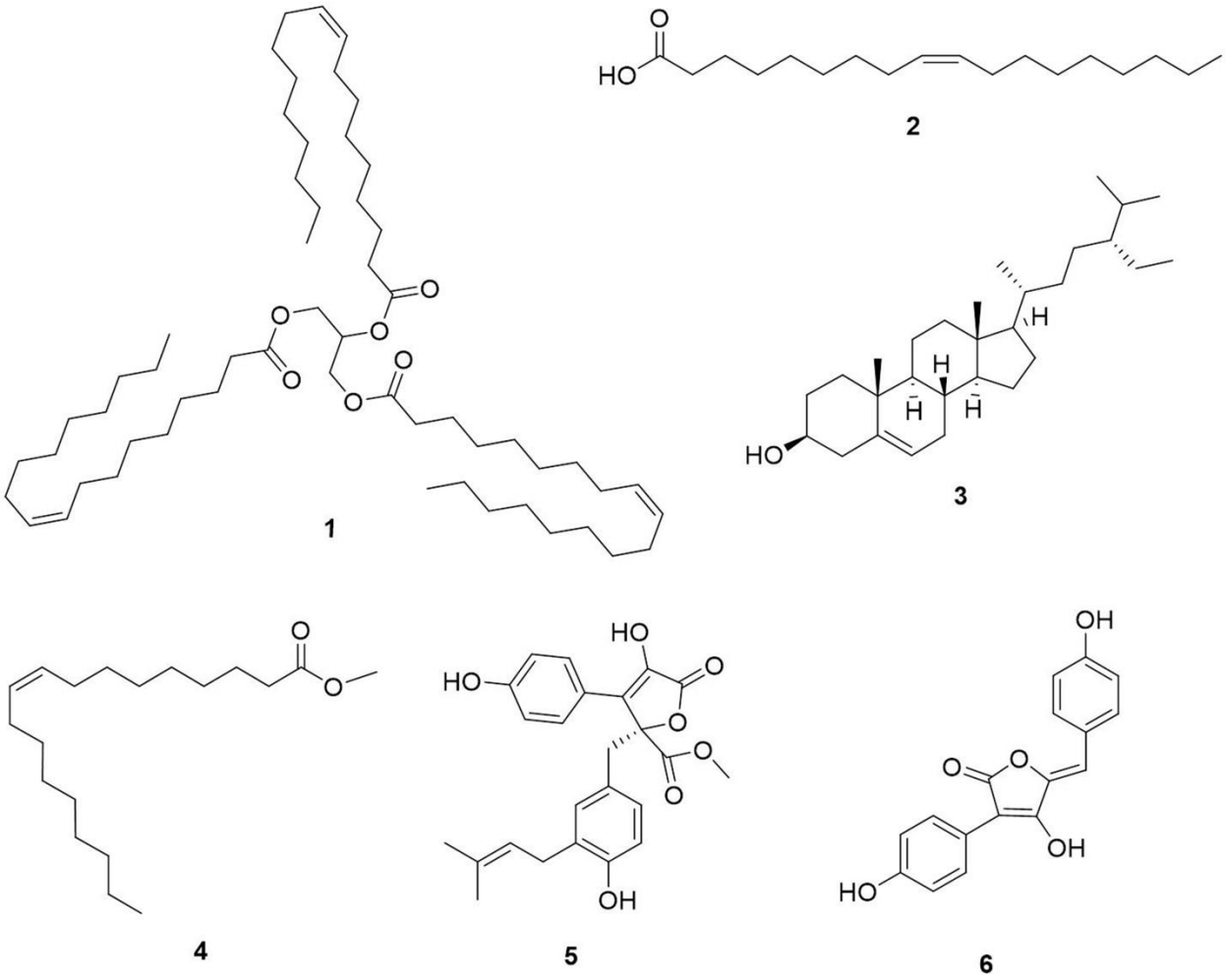

Figure 2: Chemical structures of the isolated compounds. 1: Triolein; **2:** Oleic acid; **3:** Beta-sitosterol; **4:** Methyl oleate; **5:** Butyrolactone-I; **6:** Aspulvinone E.

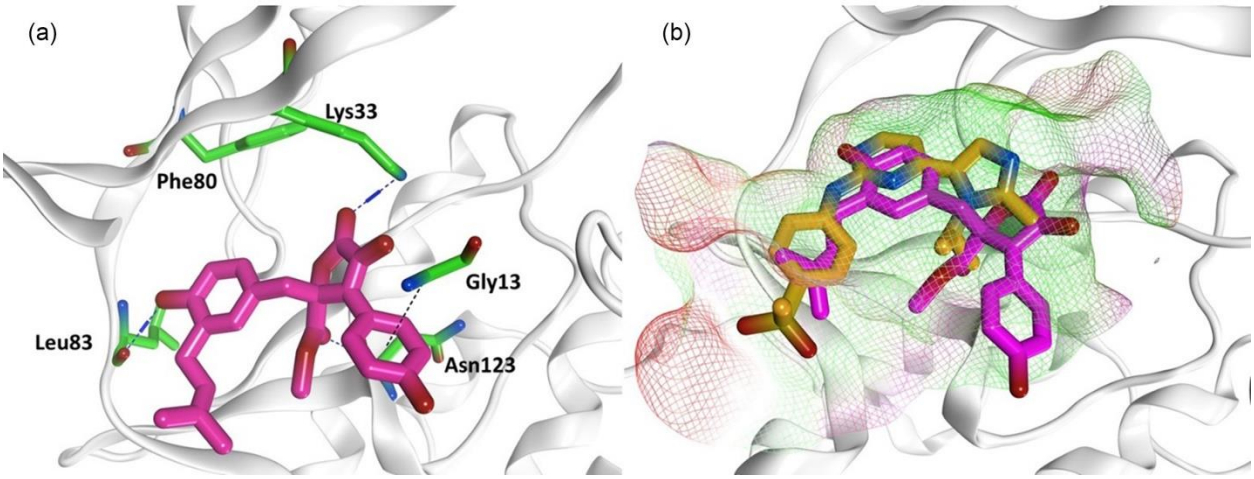

Figure 3: The top-scoring docked pose of compound 5 to the CDK2 active site (PDB ID: 6GUH). (A) Detailed binding mode of **5** (magenta) displaying hydrogen bonds (blue dashed line) and H- π interactions (black dashed line) with the key residues (green stick model). **(B)** Superimposition of the co-crystallized ligand (orange stick model) and **5** (magenta stick model).

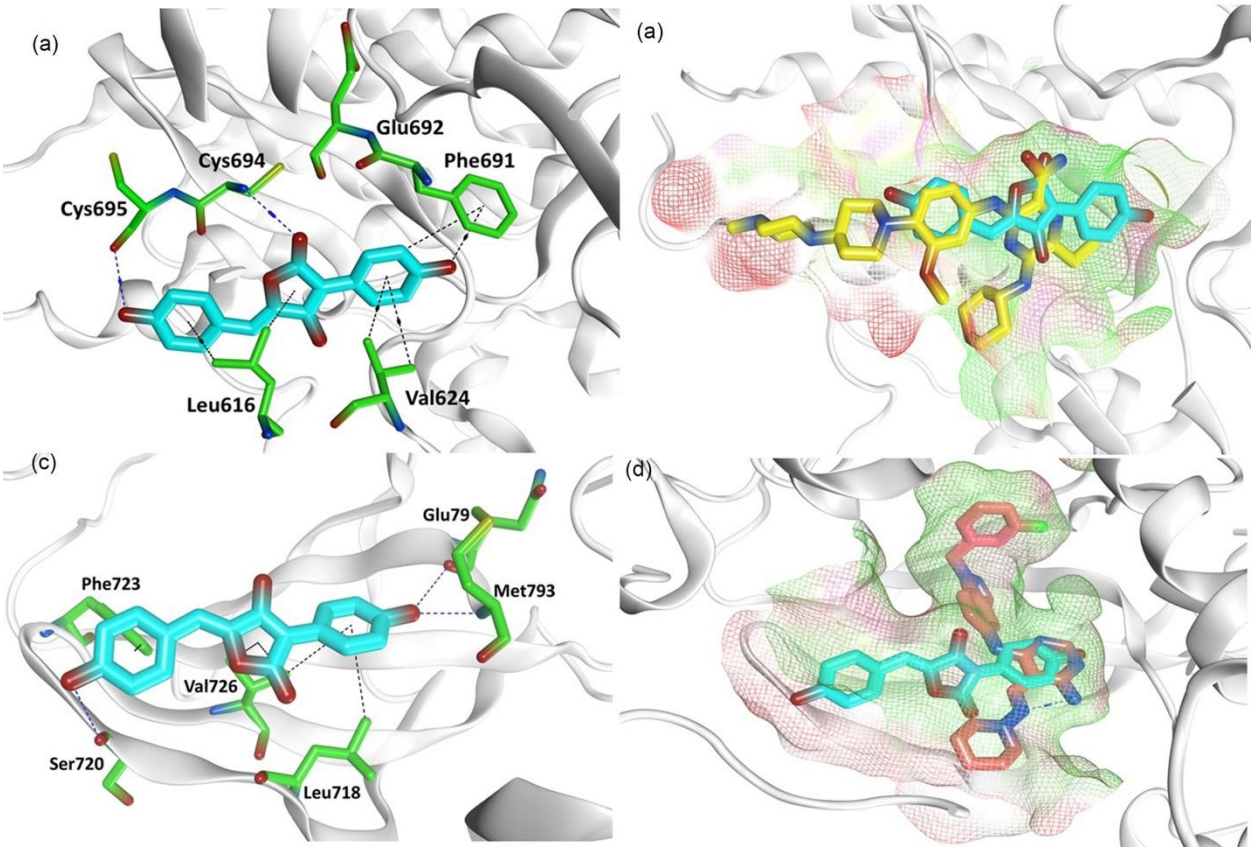

Figure 4: The top-scoring docked poses of compound 6 (PDB ID: 6JQR and 2RGP). (A) Detailed binding mode of **6** (cyan) to the FLT3 active site displaying hydrogen bonds (blue dashed line) and H-π interactions (black dashed line) with the key residues (green stick model). **(B)** Superimposition of the co-crystallized ligand (yellow stick model) and **6** (cyan stick model) to the FLT3 active site. **(C)** Detailed binding mode of **6** (cyan) to the EGFR active site displaying hydrogen bonds (blue dashed line) and H-π interactions (black dashed line) with the key residues (green stick model). **(D)** Superimposition of the co-crystallized ligand (pink stick model) and **6** (cyan stick model) to the EGFR active site.